

# On the Computation and Application of Prototype Point Patterns

Katherine E. Tranbarger Freier<sup>1</sup> and Frederic Paik Schoenberg<sup>\*,2</sup>

<sup>1</sup>Babson College Math and Science Division, 231 Forrest Street, Babson Park, MA 02457, USA

<sup>2</sup>Department of Statistics, 8125 Math-Science Building, University of California, Los Angeles, 90095-1554, USA

**Abstract:** This work addresses computational problems related to the implementation of Victor and Purpura's spike-time distance metric for temporal point process data. Three computational algorithms are presented that facilitate the calculation of spike-time distance. In addition, recommendations for penalty parameters are provided, and several properties and extensions of the spike-time metric, and of point pattern distance metrics more generally, are discussed. Applications include the formation of prototype point patterns that can be used for describing a typical point pattern in a collection of point patterns, and various clustering algorithms that can be modified for application to point process data through the use of spike-time distance and prototype patterns. Extensions of these techniques to multidimensional point patterns are also addressed.

**Keywords:** Distance metric, point process, prototype pattern.

## 1. INTRODUCTION

Temporal point process data arise naturally in the analysis of a wide variety of phenomena, including incidence of disease, sightings or births of a species, firings or neurons, or the occurrences of environmental disasters such as earthquakes, tsunamis, wildfires, and volcanic eruptions [1-4]. Often one obtains multiple realizations of a point process, and problems that arise frequently in applications include characterizing particular realizations of the point process as *outliers*, summarizing a collection of point patterns by indicating the behavior of a *typical* realization, and organizing groups of point process realizations into *clusters* of similar patterns of observations. All of these problems require the definition and computation of the distance between two point process realizations. For instance, Victor and Purpura [5] analyzed collections of neuronal firings using the spike-time distance metric between point patterns, and Schoenberg and Tranbarger [6] analyzed the behavior of typical aftershock sequences following a large earthquake using prototypes based on this spike-time metric.

Unfortunately, the spike-time metric is extremely cumbersome to compute using present methods, and this renders such applications for collections of large point process datasets infeasible. The central purpose of this paper is to develop computational algorithms for the efficient computation of spike-time distances between temporal point patterns, to enable computation of useful summaries such as the prototype of a collection of point process realizations as well as clustering, classification, and other applications of point process distance metrics.

The spike-time distance metric proposed by Victor and Purpura [5] involves the realignment, addition, and deletion

of points in point pattern X to match those in point pattern Y. The metric is somewhat analogous to several classical and well-understood distance metrics commonly used in computer imaging and other areas. For instance, Earth Mover's Distance (EMD) introduced by Rubner, Tomasi, and Guibas [7, 8] evolved from the Hitchcock solution [9] to the original transportation problem first discussed by Monge in 1781 [10]. EMD measures the amount of work required to transform a histogram of the values in one image into that of the values in another image using basic operations [8], and was shown by Levina and Bickel [11] to be equivalent to Mallows distance on probability distributions when the two image signatures in question are appropriately weighted by their sizes. In contrast to EMD, the spike-time distance of Victor and Purpura [5] focuses on matching the points of two point processes rather than the summary histograms of an image process, and thus requires some fundamentally different algorithms for its computation.

In Section 2, we review some of the mathematical history behind point pattern distance metrics and explore various properties of the spike-time metric that can aid in its computation. The primary focus of this section is dedicated to presenting three different algorithms that may be used to compute spike-time distance given repeated observations of a temporal point process. Section 3 describes point pattern prototypes along with issues relevant to their computation and approximation. Section 4 presents algorithms for clustering collections of observed point patterns based on their spike-time distances and prototype point patterns. A discussion and suggestions for further research are presented in Section 5.

## 2. SPIKE-TIME DISTANCE

Let X and Y be temporal point patterns, i.e. each is a collection of points on the real line, and corresponds to a  $\sigma$ -finite non-negative integer-valued measure on  $\mathbb{R}$  [1]. (We refer to such a collection of points as a point pattern, as

\*Address correspondence to this author at the Department of Statistics, 8125 Math-Science Building, University of California, Los Angeles, 90095-1554, USA; E-mail: frederic@stat.ucla.edu

distinguished from a point process, which is a random variable whose outcomes are point patterns).

The spike-time distance between  $X$  and  $Y$  is defined as the total cost of transforming  $X$  into  $Y$  using a series of basic movement, addition, and deletion operations [5]. Specifically, points from  $X$  can be deleted at a cost  $p_d$ , added at a cost of  $p_a$ , or moved a distance  $\Delta$  at a cost of  $p_m \Delta$ . The minimum sum of costs for the deletion, addition, and moving operations necessary to transform point pattern  $X$  into point pattern  $Y$  is the spike-time distance between  $X$  and  $Y$ . Note that in order for this to be a distance metric, it must be symmetric and thus the constraint  $p_a = p_d$  is typically imposed. While in some applications it might be desirable for  $p_a$  and  $p_d$  to take on different values, this paper focuses on the case where the spike-time distance is a symmetric distance metric. Hence in what follows we assume  $p_a = p_d$ .

One algorithm for determining the minimal sequence of deletion, addition and movement operations needed for transforming one point pattern into another is the Single-Unit (SU) algorithm discussed in Aronov [12]. We will briefly review the SU algorithm based on dynamic programming algorithms introduced by Sellers [13] and show a modification on this approach that reduces computation run time from  $O(n^2)$  to  $O(n^{4/3})$ . Also presented here is the Mutual Best Match (MBM) algorithm that is useful for determining distances between patterns of shorter lengths and which extends readily to multiple dimensions as discussed in Section 5.

### 2.1. Single-Unit Algorithm

In general, the minimal sequence of operations required to transform point pattern  $X$  into point pattern  $Y$  can be difficult to determine. In the special case where no points of  $X$  or  $Y$  are added or deleted, however, the computation is quite trivial in view of the following result that is critical in the application of all three algorithms discussed.

**Theorem 1.** Suppose that temporal point patterns  $X$  and  $Y$  each consist of exactly  $n$  points and that  $p_m \ll p_a = p_d$ , so that in effect addition and deletion of points are not permitted. Then

$$d(X, Y) = p_m \sum_{i=1}^n |x_i - y_i| \quad (1)$$

where  $x_1, x_2, \dots, x_n$  and  $y_1, y_2, \dots, y_n$  are the sorted points of  $X$  and  $Y$ , respectively.

**Proof.** The statement is trivial for  $n = 1$ . Suppose  $n = 2$ , and without loss of generality assume  $x_1 \geq y_1$ . If also  $x_2 \geq y_2$ , then  $|x_1 - y_2| + |x_2 - y_1| \geq |x_1 - y_1 + x_2 - y_2| = |x_1 - y_1| + |x_2 - y_2|$ , since both  $(x_1 - y_1)$  and  $(x_2 - y_2)$  are non-negative. Alternatively, if  $x_2 < y_2$ , then  $y_2 - x_1 \geq y_2 - x_2 > 0$ , since  $x_1 \leq x_2 < y_2$ . Similarly,  $0 \geq y_1 - x_1 \geq y_1 - x_2$ . Therefore,  $|y_1 - x_1| \leq |y_1 - x_2|$  and  $|y_2 - x_2| \leq |y_2 - x_1|$ , so  $|y_1 - x_1| + |y_2 - x_2| \leq |y_1 - x_2| + |y_2 - x_1|$ . Hence the basic operations that move the point  $x_1$  to  $y_2$  and move the point  $x_2$  to  $y_1$  have a total penalty that is at least as large as the penalties for moving  $x_1$  to  $y_1$  and moving  $x_2$  to  $y_2$ .

Now suppose  $n = k + 1$  and that the result in Theorem 1 holds for  $n = k$ . Consider any sequence of elementary operations that includes moving  $x_{k+1}$  to  $y_i$  and moving  $x_j$  to  $y_{k+1}$ , where  $i, j < k + 1$ . By the  $n = 2$  case proven above,

$|x_{k+1} - y_i| + |x_j - y_{k+1}| \geq |x_j - y_i| + |x_{k+1} - y_{k+1}|$ . That is, the elementary operations considered have cost at least as large as those obtained by moving  $x_{k+1}$  to  $y_{k+1}$  and moving  $x_j$  to  $y_i$ . Hence the minimal total cost in aligning  $X$  and  $Y$  is obtained by the elementary operations that involve moving  $x_{k+1}$  to  $y_{k+1}$ ; the cost of aligning the other  $k$  points of  $X$  with the other  $k$  points of  $Y$  is given by (1) with  $n = k$ . The result follows by induction.

Using this result, an inductive approach to spike-time distance calculation is possible. The SU algorithm of Aronov [12] determines the minimal distance between  $i = 1, 2, \dots, n$  points of pattern  $X$  and  $j = 1, 2, \dots, m$  points of pattern  $Y$  by building on the distance result for points  $i = 1, 2, \dots, n - 1$  of  $X$  and points  $j = 1, 2, \dots, m - 1$  of  $Y$ . Let  $D_{i,j}$  denote the spike-time distance between the first  $i$  points of pattern  $X$  and first  $j$  points of pattern  $Y$ . To determine the minimal distance between patterns  $X$  and  $Y$  simple calculations to complete an  $n$  by  $m$  matrix of  $D_{i,j}$  values are necessary. At each step  $D_{i,j}$  is the minimum of  $D_{i-1,j} + p_d$ ,  $D_{i,j-1} + p_d$ , and  $D_{i-1,j-1} + (p_m \times |x_i - y_j|)$  (corresponding to the options of deletion of  $x_i$ , deletion of  $y_j$ , and the pairing of  $x_i$  to  $y_j$ , respectively). In the trivial cases of  $i = 0$  or  $j = 0$ ,  $D_{i,j} = p_d \times \max(i, j)$ .

### 2.2. Modified Single-Unit Algorithm

In spike-time distance calculations, no move greater than  $(p_a + p_d)/p_m$  may take place since such a move would be greater in cost than removal and re-insertion of one of the points involved. With this fact in mind, the patterns  $X$  and  $Y$  can each be broken into patterns of shorter lengths whenever a gap of greater than  $(p_a + p_d)/p_m$  is present. In this modified SU (MSU) approach, computations involve the sorting of points  $x_1, x_2, \dots, x_n$  and points  $y_1, y_2, \dots, y_m$  combined to form one pattern,  $Z$ , of length  $n + m$ . Instances in which  $z_k - z_{k-1}$  is greater than  $(p_a + p_d)/p_m$  are easily identified to determine how  $X$  and  $Y$  can be partitioned into patterns with fewer points. For example, if such a gap was present at  $z_k = 3$ , pattern  $X_1$  would consist of all points in  $X$  less than 3 just as pattern  $Y_1$  would consist of all points in  $Y$  less than 3. The SU algorithm as earlier described is then applied to each pair of  $X_i, Y_i$  patterns formed in the partitioning process and the final distances for each pair are summed. Advantages of this modification are discussed in greater detail in Section 2.4.

### 2.3. Mutual Best Match Algorithm

In light of Theorem 1, the problem of determining the best sequence of operations to transform temporal (i.e. one dimensional) point pattern  $X$  into point pattern  $Y$  reduces to the problem of determining whether each point in the point patterns will be removed (i.e. deleted from one string or equivalently added to the other), or whether it will be kept, i.e. paired to a point in the other string. Once the points to be kept are determined, the best approach for matching the kept points in  $X$  to those in  $Y$  is simply sequential, based on Theorem 1. Evaluation of each potential set of kept points is thus remarkably straightforward. In fact, each potential distance is simply the number of points removed summed with the integrated difference between the cumulative functions associated with the remaining points in the two point patterns [6]. Given two point patterns whose spike-time distance is sought, the following results are useful in determining which points will be kept and which will be removed.

**Lemma 2.** Any point that is more than  $(p_a + p_d)/p_m = 2p_d/p_m$  away from its nearest neighbor in the alternate point pattern will be removed.

**Proof.** The proof is immediate: for such a point  $x$  in  $X$ , it is more costly to move  $x$  to a point  $y$  in  $Y$  than to delete  $x$  and add to  $X$  a point at  $y$ .

**Theorem 3.** Any pair of points  $x_i$  and  $y_j$  satisfying the following condition will be kept:

$$|x_i - y_j| < \min_{k \neq i} \{|x_k - y_j|\} < \min_{k \neq j} \{|x_i - y_k|\} < \frac{2p_d}{p_m} \quad (2)$$

**Proof.** There are three possible outcomes for points  $x_i$  and  $y_j$  satisfying the condition above. Either both points are removed, one point is kept while the other is removed, or both points are kept. We will show that the first two of these outcomes are excluded.

Suppose that both points are removed. Then the distance penalty function includes the penalty  $2p_d$  associated with those deletions. Since  $|x_i - y_j| < 2p_d/p_m$ , the penalty could be reduced by keeping both points and moving them to each other, at a cost of  $|x_i - y_j| p_m$ . Therefore, removing both  $x_i$  and  $y_j$  cannot yield the minimum penalty.

Suppose that one point is kept while the other is removed. Assume without loss of generality that  $x_i$  is kept while  $y_j$  is removed. Then  $x_i$  is paired with some point  $y_k$  such that  $y_k = y_j$  and the spike-time distance includes both penalty  $p_d$  for removal of  $y_j$  and  $|x_i - y_k| p_m$  for the move of point  $x_i$  to  $y_k$ . Since  $|x_i - y_k| > |x_i - y_j|$  the total spike-time distance penalty could be reduced by removing point  $y_k$  rather than point  $y_j$  and moving  $x_i$  to  $y_j$ . Therefore, removing one point while keeping the other cannot yield minimum penalty.

The only option that remains is that both  $x_i$  and  $y_j$  are kept in the sequence of moves yielding minimal total cost.

The Mutual Best Match (MBM) algorithm, named for the property shown in Theorem 3, uses the three discussed properties of the optimal sequence of operations in the spike-time distance metric to determine the distance between point patterns  $X$  and  $Y$ . With these properties, the problem of determining the distance between point pattern  $X$  and point pattern  $Y$  is simplified to identifying points known to be kept or deleted, then checking the total cost associated with each possible combination of potentially kept points. Calculating the total cost associated with each potential combination of kept points in the two point patterns is not computationally time prohibitive, as the sequential ordering prescribed by Theorem 1 makes this calculation extremely straightforward.

#### 2.4. Application and Penalty Selection

It is not uncommon in point process applications to observe a collection of independent point patterns resulting from a common point process of interest. An example discussed in [6] is the collection of observed aftershock sequences following strong earthquakes in distinct regions, occurring within a fixed period of time and space of each main shock. Throughout this work, we refer to such a collection of point processes simply as a point process dataset.

The number and proximity of points in each point pattern observed in a point process dataset are important to consider when determining the penalties used in the spike-time distance metric. When selecting these penalties, it is the ratio of the deletion (addition) penalty  $p_d$  to  $p_m$  that governs the setting  $p_a = p_d = 1$  and determining  $p_m$  by examining the spread of the points in the data. If  $p_m$  is too large, then little movement of points will take place in the computation of distances between point patterns, as the cost of deletion and addition will be less than most potential moves. Alternatively, if  $p_m$  is too small, then moves will be made between points that are not very close at all. With either extreme, the resulting spike-time distance will measure little more than the sum of, or difference between, the number of points in the two observed point patterns. Specifically, the spike-time distances will approach the sum of the two point pattern lengths for very large values of  $p_m$ , and will approach the absolute difference between these lengths for very small  $p_m$  values.

With these extremes in mind, one option is to set  $p_m$  to a value such that points closer than the typical inter-point distance are paired, and points further than this are removed and then reintroduced in the spike-time distance calculations. This leads to selecting penalties such that:

$$(T/M)p_m \approx 2p_d, \quad (3)$$

where  $M$  is the median number of points per observed point pattern and  $T$  is the size of the range over which the points are observed.

In simulation studies on point patterns generated from a Poisson process, the precise value of the penalties selected were shown to have little influence on the overall distribution of pattern distances. Fig. (1) shows the results from calculating the 4,950 possible pair-wise distances between 100 simulated Poisson point patterns. The results are shown for three different values of  $p_m$ : the value as determined by (3), 75% of the penalty recommended in (3), and 125% of the penalty found by (3). In each case, though the mean and standard deviation of the distances has changed (as would be expected), the distribution of distances is approximately normal for all three. Normal Q-Q plots are provided below each histogram of distances to further illustrate how closely each follows the normal distribution. Since spike-time distance is useful only for comparisons rather than as a raw measurement tool (where specific distance values have meaning out of the comparison context) the fact that the distribution of distances remains virtually unchanged in the face of rather substantial alterations to the penalty values suggests that investigations of differences and similarities of point patterns within a dataset may not be overly sensitive to the choice of penalty values, provided the penalties are within some reasonable range, at least in so far as the shape of the distribution of the distances is concerned.

Calculation time is of course a key consideration in selection of which algorithm to use with a particular data set. The main advantage of the MSU approach is that it will often require significantly less time to calculate the spike-time distance of interest. This advantage over the standard SU algorithm can be clearly seen in Fig. (2). Here, for lengths  $n = 2, 3, 4, \dots, 29, 30, 40, 50, 75, 100, 150, 200$ , distances were calculated between 1000 pairs of two

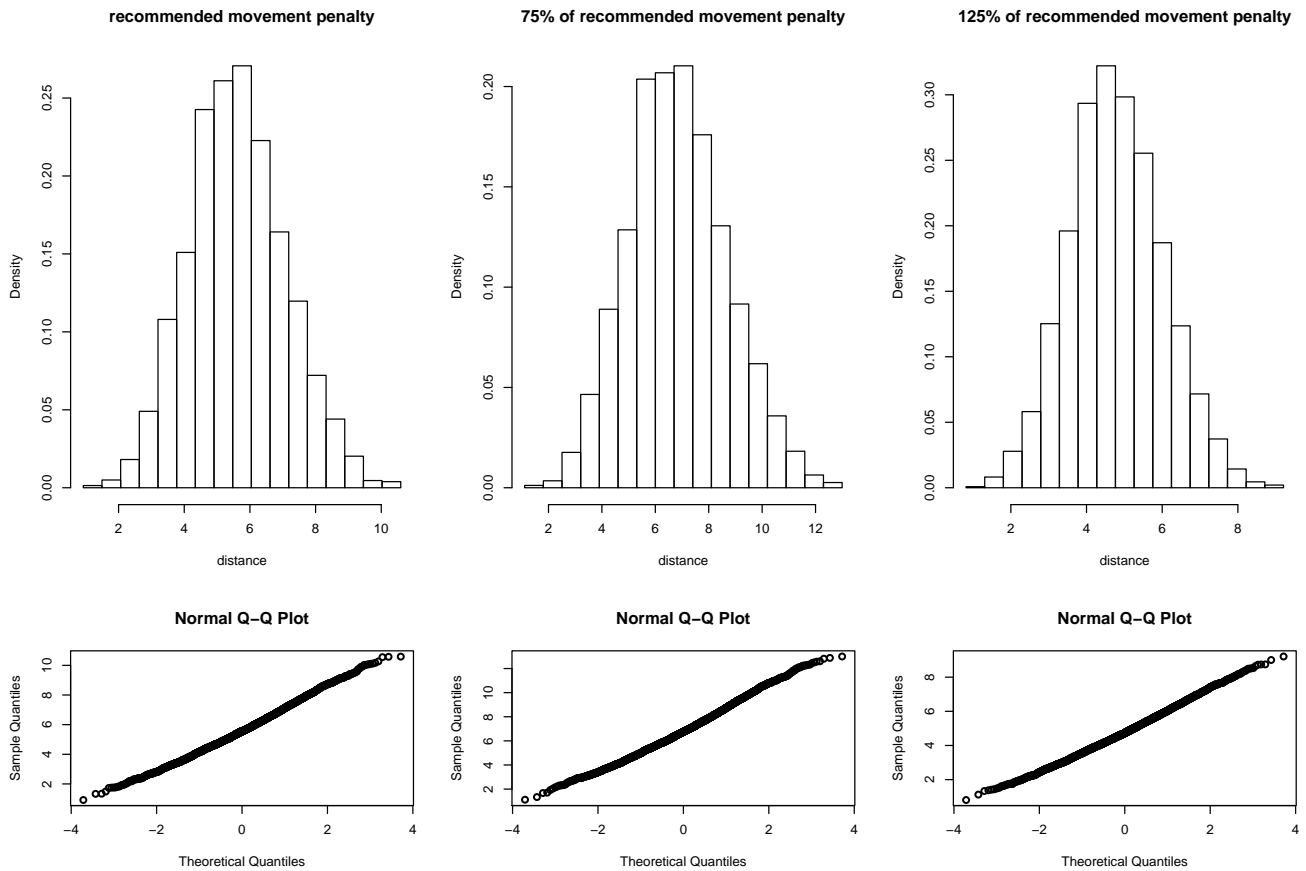


Fig. (1). Pairwise distances for 100 simulated Poisson point patterns using three different penalty values. Of note is the observation that the general shape of the distribution of distances remains normal for all three penalty values.

randomly generated patterns of  $n$  points each using both the SU and MSU algorithms programmed in R. For the modified version, additional results for  $n = 300, 400, 500$  are also shown.

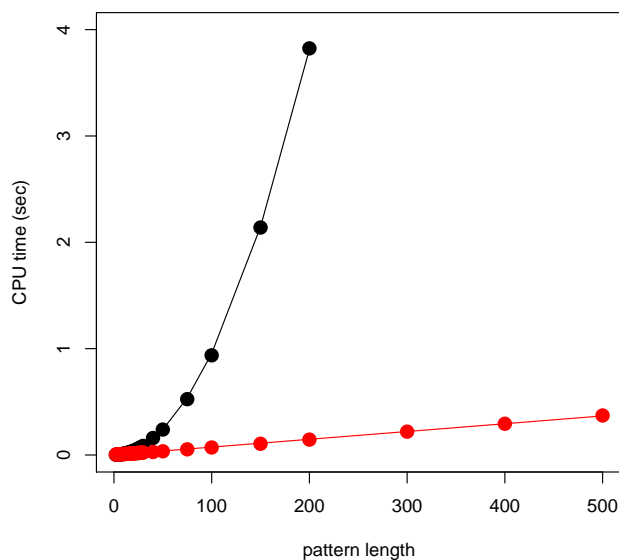


Fig. (2). Mean calculation time in R for spike-time distance as pattern length increases. The SU algorithm (in black) is shown with the best-fit  $n^2$  curve, and the MSU algorithm (in red) is shown with a linear fit.

The patterns used to create Fig. (2) were generated by taking a random sample of size  $n$  from a uniform  $(0,10)$  distribution. Points in black are the resulting mean CPU times using the standard SU algorithm. The black line included is the best fit least-squared model using  $n^2$  as the only predictor, demonstrating the  $O(n^2)$  run time achieved by the SU algorithm. Points in red are fit with a linear model and are the result from using the MSU algorithm. Though the MSU algorithm should run  $O(n^{4/3})$  due to the sorting calculation [14], up to  $n = 500$  a linear model fits the simulation results quite well as the sorting represents such a small part of all computations involved. In all cases, the penalties were fit as recommended above in (3). The ease of matrix manipulation in R is the main reason R was selected for implementation of the SU and MSU algorithms.

The run time for calculation of the spike-time distance using the MBM algorithm is approximately  $O(2^{n_1+n_2})$ , where  $n_1$  and  $n_2$  are the lengths of the two point patterns. This is because there are on the order of  $O(2^{n_1+n_2})$  combinations of points which might be kept, and each of these is examined individually. Green points in Fig. (3) illustrate this for the case  $n = n_1 = n_2$ , in which case the run time increases approximately as  $O(4^n)$ . In Fig. (3), timing simulations using the MBM approach programmed in C are included with a subset of the same results shown in Fig. (2). The overlaid green line corresponds to the best  $4^n$  fit. C was selected for the MBM algorithm because of the looping that takes place

in the MBM distance calculation. All of these computations were performed using a 1.33GHz PowerPC G4.

### 3. PROTOTYPE POINT PATTERNS

With a distance metric clearly defined, it becomes possible to identify a prototype point pattern that can be used for describing a typical observation within a point process dataset. We define this prototype to be the point pattern  $Y$  such that the sum

$$\sum_{i=1}^n d(X_i, Y) \quad (4)$$

is minimized, where  $X_i$ ,  $i = 1 \dots n$ , are the  $n$  observed point patterns in the dataset.

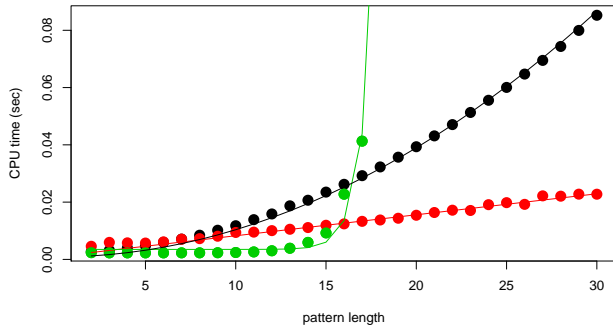


**Fig. (3).** Mean calculation time for spike-time distance as pattern length increases. The MBM distance algorithm (in C) shown in green proves to compute distances more quickly than both the SU and MSU algorithms (in R) in cases where the mean pattern length is less than 16 points (when both MBM and SU are coded in C, MBM performs better for any pattern length less than 9). For patterns of longer lengths, the MSU algorithm is shown to calculate distances most efficiently. In general, the MBM algorithm simulations follow a  $4^n$  curve, the SU algorithm (shown in black) follows a  $n^2$  curve, and the MSU algorithm (in red) is linear with increases in pattern length.

#### 3.1. Basic Properties of Prototype Points

A convenient feature making prototypes easy to identify is described in Theorem 4. Before stating this theorem, we first turn to the definition of the median of a sorted list of numbers  $z = \{z_1, z_2, \dots, z_m\}$ , whose length  $m$  is even. Many texts define the median of such a list as the mean of the two entries  $z_{m/2}$  and  $z_{m/2+1}$ . Instead, let us refer to any value  $M$  such that  $z_{m/2} \leq M \leq z_{m/2+1}$  as a median of  $z$ .

With this convention in mind, we return to the problem of determining prototypes. Suppose that  $Y$  is the prototype of a point process dataset consisting of  $n$  point patterns  $X_1, \dots, X_n$ . For any point  $p$  in the prototype, consider the collection of points in the point process dataset  $z_p = \{z_1, z_2, \dots, z_m\}$  to which  $p$  is paired. That is, each element of  $z_p$  is associated with a different  $X_i$  point pattern within the complete dataset and specifically, each point  $z_i$  is the point to which point  $p$  is moved to when the spike-time distance between  $Y$  and  $X_i$  is determined. Note that  $m \leq n$ , since  $p$  might not be kept in the spike-time distance between the prototype and some of the point patterns in the dataset.

**Theorem 4.** Any point  $p$  in the prototype is a median of  $z_p$ .

**Proof.** Fix any prototype point  $p$  and the list  $z_p = \{z_1, \dots, z_m\}$  of points in the dataset to which  $p$  is paired. Note that, in order for  $p$  to be a point of the prototype, the sum of distances from  $z_i$  to  $p$  must be less than or equal to the sum of distances from  $z_i$  to any other point  $q$ . Let  $q$  be a median of  $z_p$ , and suppose that  $p$  is not a median of  $z_p$ . We will show that the sum of distances from  $z_i$  to  $q$  is less than the sum of distances from  $z_i$  to  $p$ , contradicting the assumption that  $p$  is a point of the prototype.

First suppose that the length  $m$  of  $z_p$  is odd, and without loss of generality assume  $p < q$ . The sum of all  $m$  distances from  $z_i$  to  $q$  is:

$$= \sum_{i=1}^{(m-1)/2} |z_i - q| + \sum_{i=(m+3)/2}^m |z_i - q| \quad (5)$$

since  $|z_{(m+1)/2} - q| = 0$ . The sum of the  $m$  distances from  $z_i$  to  $p$  is:

$$\begin{aligned} \sum_{i=1}^m |z_i - p| &= \sum_{i=1}^{(m-1)/2} (|z_i - q| - (q - p)) + \sum_{i=(m+3)/2}^m (|z_i - q| + (q - p)) + (z_{(m+1)/2} - p) \\ &= \sum_{i=1}^m |z_i - q| - \left(\frac{m-1}{2}\right)(q - p) + \left(\frac{m-1}{2}\right)(q - p) + (z_{(m+1)/2} - p) \\ &= \sum_{i=1}^m |z_i - q| + (z_{(m+1)/2} - p) \end{aligned} \quad (6)$$

Therefore, the sum of distances from  $z_i$  to  $p$  in (6) is greater than the sum of distances to  $q$ , which is a contradiction. If  $m$  is even, then without loss of generality assume that  $p < z_{m/2}$ . The sum of all  $m$  distances from  $z_i$  to  $q$  is:

$$\begin{aligned} \sum_{i=1}^m |z_i - q| &= \sum_{i=1}^{(m/2)-1} (|z_i - z_{(m/2)}| + (q - z_{(m/2)})) \\ &+ \sum_{i=(m/2)}^{(m/2)+1} (|z_i - q|) + \sum_{i=(m/2)+2}^m (|z_i - z_{(m/2)+1}| + (z_{(m/2)+1} - q)) \\ &= \sum_{i=1}^{(m/2)-1} (|z_i - z_{(m/2)}|) + (z_{(m/2)+1} - z_{(m/2)}) + \\ &\sum_{i=(m/2)+2}^m (|z_i - z_{(m/2)+1}|) + \left(\frac{m}{2}\right) \times (z_{(m/2)+1} - z_{(m/2)}) \end{aligned} \quad (7)$$

and the sum of distances from  $z$  to  $p$  is:

$$\begin{aligned} \sum_{i=1}^m |z_i - p| &= \sum_{i=1}^{(m/2)-1} (|z_i - z_{(m/2)}| - (z_{(m/2)} - p)) + \\ &\sum_{i=(m/2)}^{(m/2)+1} (|z_i - p|) + \sum_{i=(m/2)+2}^m (|z_i - z_{(m/2)+1}| + (z_{(m/2)+1} - p)) \\ &= \sum_{i=1}^{(m/2)-1} (|z_i - z_{(m/2)}|) + (z_{(m/2)+1} - z_{(m/2)}) + (z_{(m/2)} - p) + \\ &\sum_{i=(m/2)+2}^m (|z_i - z_{(m/2)+1}|) + \left(\frac{m}{2} - 1\right) \times (z_{(m/2)+1} - z_{(m/2)}) \end{aligned}$$

$$= \sum_{i=1}^m |z_i - q| + (z_{m/2} - p) \tag{8}$$

which again contradicts the assumption that  $p$  is a point of the prototype.

A consequence of Theorem 4 is that, for any point process dataset, there exists a prototype comprised entirely of points observed in the dataset. That is, in searching for a prototype, one may limit one's search to all possible combinations of entries in the dataset.

### 3.2. Prototype Determination

In addition to the result shown in Theorem 4, note that each point of the prototype must be within  $(p_a + p_d)/p_m$  of a fraction  $p_a / (p_a + p_d)$  of the dataset's point patterns, as discussed in [6]. Let  $n$  be the number of point patterns in the dataset. Then each point  $z$  for which at least  $np_a / [2(p_a + p_d)]$  other points from distinct point patterns in the dataset are in the range  $[z - (p_a + p_d)/p_m, z]$  and at least  $np_a / [2(p_a + p_d)]$  other points from distinct point patterns in the dataset fall in the range  $[z, z + (p_a + p_d)/p_m]$  is a candidate for inclusion in the prototype. For the case where  $p_a = p_d$ , this is simply  $n/4$  points from distinct point patterns in the dataset occurring on either side of  $z$ , within a distance  $2 * p_d / p_m$ . In practice, this observation will likely significantly decrease the number of candidates to be considered as potential points in the prototype.

#### 3.2.1. Direct Algorithms for Prototype Determination

With a finite number of candidate prototype points ( $n_{cp}$ ) to consider, one may compute the sum in equation (4) for each possible prototype, i.e. each possible collection of points that are potentially in the prototype. For sufficiently small movement penalties, the prototype will generally have length equal to the median length  $M$  of the  $n$  point patterns,

so one may limit one's search the  $\binom{n_{cp}}{M}$  collections of length

$M$  as candidates for the prototype. Depending on the size of the dataset of interest, this may be a reasonable task to undertake. Alternatively, if  $p_m$  is not small enough to allow for a prototype of length  $M$ , then the best prototype of length  $k$  can be iteratively sought for  $k = 1, 2, \dots, M$ . In this case, the prototype may be found by considering the optimal prototype candidate of length  $k = 1$  and progressively increasing  $k$ , ending the search once the sum in (4) for length  $k + 1$  is greater than the sum (4) for the best prototype of length  $k$ .

#### 3.2.2. Forward and Reverse Stepwise Approximation

Finding the prototype of a set of point patterns as prescribed in Section 3.2.1 may prove to be prohibitively tedious for datasets with a large number of point patterns, or for point patterns with a large median number of points. In this case, stepwise methods can be implemented to attain an approximate prototype solution.

A reverse stepwise approach can be implemented by first finding the optimal prototype of median length  $M$ . Possible prototypes of shorter length can then be found by eliminating points from the length  $M$  prototype one at a time. This strategy continues until the optimal prototype of length  $k - 1$

has a larger sum of distances (4) than the best prototype candidate of length  $k$ .

While the reverse stepwise approach will entail fewer computations than finding the prototype directly, even the reverse stepwise approximation can prove prohibitively cumbersome due to the long length of the prototype computed in the first stage. An alternative is to use a forward stepwise approach, which can further reduce computation time by beginning with a short prototype candidate and progressively expanding it by one point at each step. In each iteration, the sum of pattern-prototype distances (4) for the prototype candidate of length  $k$  is compared with the sum for the prototype candidate of length  $k - 1$ .

Fig. (4) illustrates the speed of the forward stepwise prototype approximation approach using the MBM algorithm for distance calculations, again using a 1.33GHz PowerPC G4 processor. Here,  $N = 5, 10, \dots, 50$  Poisson processes of mean length  $n = 1, 2, \dots, 10$  were simulated and the prototypes of the  $N$  patterns were determined using the forward stepwise algorithm. Mean CPU times were recorded after 100 repetitions at each level of  $N$  and  $n$ . As seen in Fig. (4), the number of point patterns in a dataset and the average length of those patterns have quite different effects on the calculation time required for prototype determination. While the large perspective plot of Fig. (4) shows these two factors together, the two smaller plots to the right illustrate the factors' effects on time separately by averaging the results first over the  $N$  levels of number of point patterns and secondly for the  $n$  levels of pattern mean length. These marginal plots show that while the mean pattern length has a relationship to run time very similar to that seen in Fig. (3) for the time required for MBM distance calculations, the relationship between the number of point patterns and run time is nearly linear. This result is not surprising in light of the fact that collections of longer point patterns will have a prototype longer in length than collections of shorter point patterns. Longer prototypes require additional steps in the stepwise algorithm and the CPU time required for each step increases rapidly as the algorithm continues.

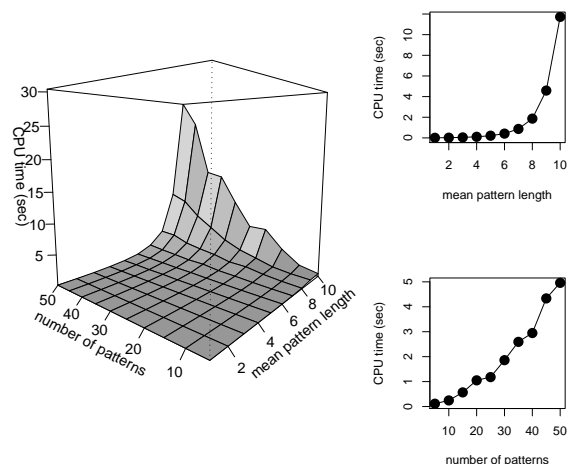


**Fig. (4).** CPU time for forward stepwise prototype approximation of simulated Poisson point patterns of varying length and number. Distances within the prototype algorithm were computed using the MBM algorithm.

### 3.3. Penalty Selection Considerations

Penalties selected for  $p_m$ ,  $p_a$ , and  $p_d$  play a significant role in prototype determination. As stated in section 3.2, a point at time  $t$  can only be part of the prototype if at least  $p_a / (p_a + p_d)$  of the point patterns in the dataset contain a point within the interval  $(t - 2p_a / p_m, t + 2p_a / p_m)$ . Selection of moving penalties that are too large will lead to prototypes that seem unusually short, since the range  $t \pm 2p_a / p_m$  will be quite small.

When the primary purpose of the prototype pattern is to serve as an example of a typical point pattern, it is useful to set  $p_m$  to be quite small compared to what might be advisable for distance calculations. Setting  $p_m$  to a small positive value when  $p_a = p_d$  enables the prototype to take on the median number of points in the dataset. Because each prototype point must be matched to points within at least  $p_a / (p_a + p_d)$  of the observed point patterns, it is typically not possible to achieve a prototype of greater than median length while maintaining the  $p_a = p_d$  restriction.

Fig. (5) illustrates how the length of the prototype is related to the relative size of the selected  $p_m$  and  $p_a = p_d$  values. For the first plot on the left, prototypes were calculated for 100 simulated datasets, each consisting of 20 stationary Poisson processes of rate 1 on  $(0, T)$ , using the forward stepwise algorithm and 100 different  $p_m$  values ranging from 0.001 to 2.0. In all cases,  $p_a = p_d = 1$ . The mean prototype length for each penalty value is seen along the y-axis and is plotted against the corresponding movement penalty value. As expected, smaller values of  $p_m$  correspond to longer prototype lengths, with a leveling off across very small  $p_m$  values where the maximum prototype length (the median) has been achieved.

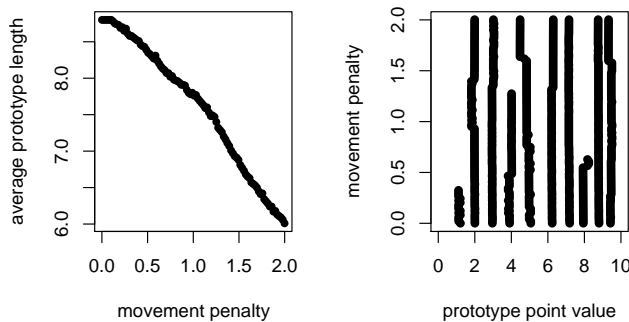


**Fig. (5).** On the left it is seen that as movement penalty values increase, the resulting prototype pattern decreases in length. The graph at right shows changes in the movement penalty have little influence over location of prototype points. While length decreases with increasing movement penalties, the general location of prototype points is largely consistent across all reasonable penalty values. Plotted are the prototype points for a simulated dataset of 20 Poisson patterns of rate 1 ranging in time from 0 to 10 computed using  $p_a=p_d=1$  and  $0.01 \leq p_m \leq 2$  as plotted on the y-axis.

The plot on the right of Fig. (5) shows the 100 prototypes calculated for one randomly selected simulated dataset used for the illustration on the left. Of particular interest is the observation that while the number of points in the prototype decreases with increases in  $p_m$ , the actual location of many of the prototype points remains essentially constant across a wide range of penalty values. This suggests that for any particular dataset, the locations of the points in the prototype

will be rather robust to choices of  $p_m$  and  $p_a = p_d$ . Small changes in the ratio  $p_m / p_a$  appear to have surprisingly little effect on either the prototype pattern or the overall distribution of distances as seen earlier in Fig. (1).

## 4. CLASSIFICATION THROUGH CLUSTERING

Using the spike-time distance metric and prototype, various clustering algorithms established for standard multivariate data can be modified for use in point process applications. This section describes how three such methods can be adapted and discusses issues in the selection of addition, deletion, and movement penalties when these clustering algorithms are used.

### 4.1. HMEANS, KMEANS and Agglomerative Clustering

HMEANS and KMEANS clustering are two closely related iterative techniques useful for clustering multi-variate data. Both HMEANS and KMEANS clustering begin by randomly assigning each observation to one of  $c$  clusters and finding the center of each cluster. While cluster centers are conventionally defined as centroids in standard HMEANS and KMEANS clustering of multivariate data [15], one may instead use the prototype as the definition of the center of a cluster of point patterns when analyzing a point process dataset.

A third option is an agglomerative approach that assigns each observed point pattern to its own cluster and then systematically combines clusters. This approach is especially useful in cases where HMEANS and KMEANS fail to converge after numerous iterations.

With each observed point pattern assigned to a cluster of its own, each cluster's prototype is simply the member pattern. The pair-wise distances between each cluster prototype can be found and the nearest two clusters joined to form one larger two-pattern cluster. From here, the new cluster prototype is determined, and the new pair-wise distances between prototypes are calculated. The process repeats until only  $c$  desired clusters remain. If the amount of data makes computing all pair-wise distances unfeasible, a similar approach is to consider pair-wise distances for only one point pattern at a time in either a randomly assigned order, or in order of length from the longest pattern to the shortest. Our investigations suggest that this procedure of ordering the point patterns from longest to shortest and then progressively merging the point patterns minimizes problems that can occur if the  $p_a$ ,  $p_d$ , and  $p_m$  penalties are set such that pattern length overshadows other features in the distance measures.

### 4.2. Penalty Choice Considerations

While setting  $p_m$  to a small value is useful in determining prototypes, very small  $p_m$  values are not desirable in clustering applications. As discussed in Section 2.4, small penalties for movement of points will lead to distances that approach the absolute difference in pattern lengths, while large movement penalties lead to distance calculations that approach the sum of point pattern lengths. In clustering, either extreme will lead to clusters assigned by grouping patterns of similar lengths rather than patterns with similarly placed points. For the simulation presented in Fig. (6), ten point patterns were created for each of two different

methods. Ten realizations of a rate 1 Poisson process on (0,6), and another ten point patterns were each created by sampling  $n$  points independently from a normal random variable with mean 3.0 and standard deviation 0.25, where  $n$  is a Poisson random variable with mean 6.0. Patterns of length zero were excluded. Plotted in Fig. (6) is the mean failure rate for HMEANS in correctly identifying the two different types of patterns over 125 simulations. The mean rate of failure is shown for twenty different  $p_m$  values ranging from 5% to 200% of the penalty recommended in (3) for distance calculations. It is clear in these results that extremely small values of  $p_m$  are less successful at clustering than values similar to that advised in (3) for distance measurements.

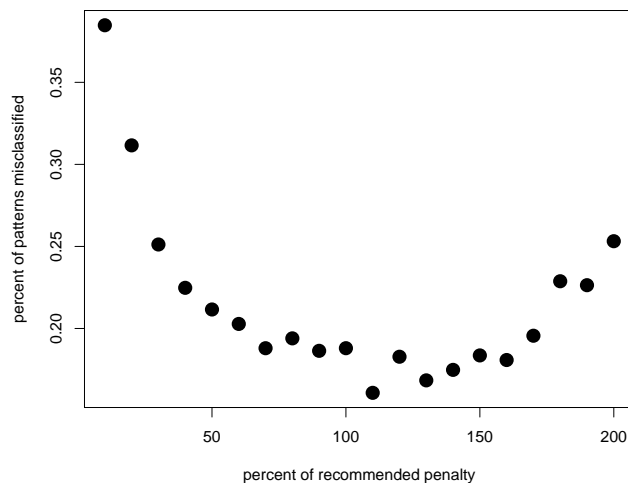


**Fig. (6).** For this simulation (repeated 125 times) ten patterns were created following a Poisson process model of rate 1 with a mean length of six points and ten patterns were created by randomly sampling from a Normal (3, 0.25) distribution of a size determined by a Poisson(6) random variable. As shown, extremely small penalty values cause HMEANS to incorrectly classify patterns more frequently than penalty values closer to that recommended in (3) of Section 2.4.

## 5. MULTI-DIMENSIONAL EXTENSIONS AND DISCUSSION

The spike-time distance metric as examined in this work, and as originally proposed by Victor and Purpura, has thus far been applied primarily to temporal point patterns [16] as defined in Section 2. This is just the beginning of ways prototypes and the spike-time metric can be used though as the spike-time metric, the related prototype pattern technique, and related clustering algorithms can all be extended to point process data with points occurring in  $\mathbf{R}^d$ .

In the extension of the definition of the spike-time distance metric to  $\mathbf{R}^d$ , points can be added with penalty  $p_a$ , deleted with penalty  $p_d$ , or moved along the  $i^{\text{th}}$  axis a distance of  $\Delta$  at a cost of  $p_m^{(i)} \Delta$ . Moving penalties  $p_m^{(1)}, p_m^{(2)}, \dots, p_m^{(d)}$  may be set independently for movement along each of the  $d$  axes as in (3) for distance calculations and clustering application settings. As with the one-dimensional case, smaller values for movement penalties are again useful for prototype determination to enable longer length prototype

point patterns. While the ratio of  $p_a$  and  $p_d$  to moving penalty  $p_m$  was of primary importance for temporal point process work, the relative values of the  $d$  movement penalties must also be considered when multiple dimensions are involved. These ratios must be considered so as to avoid (or allow) inter-point distances along one or more dimensions being more heavily weighted in distance calculations. As might be expected, spike-time distance calculations are far more cumbersome in  $\mathbf{R}^d$ , as the result of Theorem 1 does not hold in more than one dimension. Without the result of Theorem 1, neither the SU nor MSU approaches can be implemented. Also, using MBM, multiple pairing arrangements must be considered for each possible set of kept points. The process to determine which points will be kept and which will be removed under the MBM algorithm remains unchanged as Lemma 2 and Theorem 3 extend immediately to multiple dimensions.

For prototype pattern determination, a modified version of Theorem 4 applies to the multi-dimensional setting. With more than one dimension, rather than each prototype point  $p$  being a median of the points  $(z_1, z_2, \dots, z_m)$  it is paired with, each coordinate of prototype point  $p$  will be a median of the corresponding coordinate of the points  $(z_1, z_2, \dots, z_m)$ . Therefore, while the prototype may not contain points in the dataset, there exists a prototype made entirely of points such that each coordinate of each prototype point is a coordinate of one of the points observed in the dataset.

Clustering algorithms discussed in Section 4 can be applied to multi-dimensional point pattern data without modification. For some datasets, the computation time involved in prototype determination impedes the use of the clustering algorithms as described in Section 4 and slight modifications can be made, such as considering only one of the  $d$  dimensions at a time in each step of the prototype and/or distance calculation. Such a monothetic approach is used in [6] for clustering earthquake aftershock activity considering the time, magnitude, and location of each aftershock one at a time.

While the spike-time distance metric is only one of countless distance metrics for point pattern data [5], the concept of a prototype sequence is one that exists independently of distance metric specifics. Therefore, though many of the results presented here apply solely to the spike-time metric, the approaches to determining prototypes and clusters derived from the ability to measure distances between point patterns should remain useful in conjunction with other point pattern distance metrics.

## ACKNOWLEDGEMENTS

We thank Chuck Woody for introducing us to the work of Victor and Purpura, and we thank Pepe Segundo for introducing us to Chuck Woody. This material is based upon work supported by the National Science Foundation under Grant No. 0306526. Any opinions, findings, and conclusions or recommendations expressed in this material are those of the authors and do not necessarily reflect the views of the National Science Foundation. This research was also supported by the Southern California Earthquake Center. SCEC is funded by NSF Cooperative Agreement EAR-



0529922 and USGS Cooperative Agreement 07HQAG0008. The SCEC contribution number for this paper is 1283.

## REFERENCES

- [1] D. Daley, and D. Vere-Jones, *An Introduction to the Theory of Point Processes, Vol.1: Elementary Theory and Methods*, 2nd ed. Springer-Verlag: New York, 2003.
- [2] F.P. Schoenberg, D.R. Brillinger, and P.M. Guttorp, "Point processes, spatial-temporal". A. El-Shaarawi and W. Piegorisch, Eds., in *Encyclopedia of Environmetrics*, Wiley, NY, 2002, vol. 3, pp. 1573-1577.
- [3] P. Guttorp and M. Thompson, "Nonparametric estimation of intensities for sampled counting processes," *J. R. Stat. Soc., Series B* 52, pp. 157-173, 1990.
- [4] D.L. Synder, and M.I. Miller, *Random Point Processes in Time and Space*. Wiley: New York, 1991.
- [5] J. Victor, and K. Purpura, "Metric-space analysis of spike trains: theory, algorithms and application", *Network: Comput. Neural Syst.* vol. 8, pp. 127-164, 1997.
- [6] F.P. Schoenberg, and K.E. Tranbarger, "Description of earthquake aftershock sequences using prototype point processes", *Environmetrics* vol. 19, pp. 271-286, 2008.
- [7] Y. Rubner, C. Tomasi, and L. Guibas, "A Metric for Distributions with Applications to Image Databases", in *IEEE Int. Conf. Comput. Vis*1998, pp. 59-66,
- [8] Y. Rubner, C. Tomasi, and L. Guibas, "The earth mover's distance as a metric for image retrieval", *Int. J. Comput. Vis.*, vol. 40(2), pp. 99-121, 2000.
- [9] F. L. Hitchcock, "The distribution of a product from several sources to numerous localities", *J. Math. Phys.*, vol. 20, pp. 224-230, 1941.
- [10] G. Monge, *M'emoire sur la Th'eorie des D'eblais et des Remblais*, Histoire de l'Acad'emie Royale des Sciences: Paris, 1781.
- [11] E. Levina, and P.J. Bickel, "The Earth Mover's Distance is the Mallows Distance: Some Insights from Statistics", *Proceedings of ICCV Vancouver*, Canada, 2001, pp. 251-256.
- [12] D. Aronov, "Fast algorithm for the metric-space analysis of simultaneous responses of multiple single neurons" *J. Neurosci. Methods*, vol. 124, pp. 175-179, 2003.
- [13] P.H. Sellers, "On the theory and computation of evolutionary distances" *SIAM J. Appl. Math.* vol. 26, pp. 787-793, 1974.
- [14] R. Sedgewick, "A new upper bound for Shell sort", *J. Algorithms* vol. 7, pp. 159-173, 1986.
- [15] H. Spath, *Cluster Analysis Algorithms for Data Reduction and Classification of Objects*, E. Horwood, Chichester and Halsted Press: New York, 1980.
- [16] D. Reich, F. Mechler, K. Purpura, and J. Victor, "Interspike intervals, receptive fields and information encoding in primary visual cortex", *J. Neurosci.*, vol. 20, no. 5, pp. 1964-1974, 2000.

Received: April 6, 2009

Revised: May 26, 2009

Accepted: November 3, 2009

© Freier and Schoenberg; Licensee *Bentham Open*.

This is an open access article licensed under the terms of the Creative Commons Attribution Non-Commercial License (<http://creativecommons.org/licenses/by-nc/3.0/>) which permits unrestricted, non-commercial use, distribution and reproduction in any medium, provided the work is properly cited.